Environmental Pollution 239 (2018) 757–767

Contents lists available at ScienceDirect

Environmental Pollution

journal homepage: www.elsevier.com/locate/envpol

Total mercury and methylmercury accumulation in wild plants grown at wastelands composed of mine tailings: Insights into potential candidates for phytoremediation☆

Xiaoli Qian [a], Yonggui Wu [a], Hongyun Zhou [a], Xiaohang Xu [b], Zhidong Xu [b], Lihai Shang [b], Guangle Qiu [b, *]

[a] College of Resources and Environmental Engineering, Guizhou University, Guiyang, 550003, PR China
[b] State Key Laboratory of Environmental Geochemistry, Institute of Geochemistry, Chinese Academy of Sciences, Guiyang, 550081, PR China

ARTICLE INFO

Article history:
Received 8 January 2018
Received in revised form
20 April 2018
Accepted 23 April 2018
Available online 2 May 2018

Keywords:
Total mercury and methylmercury
Wild plant species
Bioconcentration factors
Phytoremediation
Wastelands

ABSTRACT

Total mercury (THg) and methylmercury (MMHg) were investigated in 259 wild plants belonging to 49 species in 29 families that grew in heavily Hg-contaminated wastelands composed of cinnabar ore mine tailings (calcines) in the Wanshan region, southwestern China, the world's third largest Hg mining district. The bioconcentration factors (BCFs) of THg and MMHg from soil to roots ($[THg]_{root}/[THg]_{soil}$, $[MMHg]_{root}/[MMHg]_{soil}$) were evaluated. The results showed that THg and MMHg in both plants and soils varied widely, with ranges of 0.076–140 μg/g THg and 0.19–87 ng/g MMHg in roots, 0.19–106 μg/g THg and 0.06–31 ng/g MMHg in shoots, and 0.74–1440 μg/g THg and 0.41–820 ng/g MMHg in soil. Among all investigated species, *Arthraxon hispidus, Eremochloa ciliaris, Clerodendrum bunge, and Ixeris sonchifolia* had significantly elevated concentrations of THg in shoots and/or roots that reached 100 μg/g, whereas *Chenopodium glaucum, Corydalisedulis maxim, and Rumex acetosa* contained low values below 0.5 μg/g. In addition to the high THg concentrations, the fern *E. ciliaris* also showed high BCF values for both THg and MMHg exceeding 1.0, suggesting its capability to extract Hg from soils. Considering its dominance and the tolerance identified in the present study, *E. ciliaris* is suggested to be a practical candidate for phytoextraction, whereas *A. hispidus* is identified as a potential candidate for phytostabilization of Hg mining-contaminated soils.

1. Introduction

Mercury (Hg) is a highly toxic trace element that can be accumulated and biomagnified at high trophic levels via food chains (Lindqvist, 1991; Clarkson, 1993; Lindberg et al., 2007; Xia et al., 2010). The toxicity and mobility of Hg are dependent on its chemical forms in the environment. Methylmercury (MMHg), an organic form produced by anaerobic bacteria acting on inorganic Hg (IHg) under certain conditions, is the most toxic Hg species because of the accumulation and biomagnification in biota (WHO, 1990). Compared with other Hg forms, MMHg is effectively taken up and absorbed by organisms, with bioconcentration factors (BCFs) ranging from 10^4 to 10^7 (Stein et al., 1996), thereby posing an increased risk to human health and wildlife. The Minamata disease that occurred in Japan was caused by the consumption of fish and other seafood contaminated by MMHg.

Mercury mines are one of the persistent anthropogenic Hg sources to the environment. Historic mining and retorting of cinnabar ores release much elemental Hg (Hg^0) and water-soluble Hg compounds into nearby surroundings (e.g. Gray et al., 2004; Qiu et al., 2005, 2013), and may also generate numerous wastelands composed of Hg-enriched mine tailings (calcines) adjacent to abandoned retorts and adits. In China, significant quantities of Hg-enriched wastelands are found in the Wanshan Hg mining region, the largest national metallic Hg products center in Guizhou Province, of which cinnabar ore mining and retorting activities may date back to 221 BCE. Mercury concentrations in the calcines have been recorded as high as 4400 μg/g (Qiu et al., 2005), which are continuously releasing Hg downstream in the region. Hence, the

☆ This paper has been recommended for acceptance by Dr. Jorg Rinklebe.

* Corresponding author. State Key Laboratory of Environmental Geochemistry, Institute of Geochemistry, Chinese Academy of Sciences, 99 Lincheng West Rd., Guiyang, 550081, PR China.
E-mail address: qiuguangle@vip.skleg.cn (G. Qiu).

https://doi.org/10.1016/j.envpol.2018.04.105
0269-7491/

wastelands that are composed of amounts of calcines have become major Hg sources to the surrounding ecosystems after the Hg mines have been abandoned for several decades (Gosar and Žibret, 2011; Tomiyasu et al., 2012), releasing Hg^0 and secondary Hg compounds via natural weathering and runoff into air, soil, and water that enter biota (Kocman et al., 2011).

Previous studies show that plant roots can uptake Hg from soil and transfer it to shoots, but the efficiency largely depends on the Hg form and its bioavailability in the soil solution (Baya and Van Heyst, 2010; Millán et al., 2006; Pérez-Sanz et al., 2012; Lu et al., 2016). Bioavailable Hg in soils varies with time and is usually operationally defined by various laboratory extraction procedures (Beckers and Rinklebe, 2017). Extractants such as water, ammonium thiosulfate, and neutral salts supposedly quantify the so-called bioavailable Hg fraction in soils (e.g. Menzies et al., 2007; Frohne and Rinklebe, 2013; Fernández-Martínez and Rucandio, 2013; Zhu et al., 2015). Generally, the highly toxic MMHg species are more easily taken up and transferred by roots from soils to shoots than IHg (Bishop et al., 1998; Gnamuš et al., 2000; Schwesig and Krebs, 2003; Rajan et al., 2008; Shiyab et al., 2009). Plants can also uptake Hg^0 from the atmosphere by direct adsorption through the leave stomata (Patra and Sharma, 2000), or via foliar uptake from atmospheric deposition (Millhollen et al., 2006). The process of Hg^0 reemitting from leaves to the atmosphere can also occur (Fay and Gustin, 2007). Total mercury (THg) concentrations in plants from uncontaminated control sites are usually less than 0.1 μg/g (Lindqvist et al., 1991), but are abnormally high in plants growing in abandoned Hg-mining regions (Higueras et al., 2006; Zhao et al., 2014; Fernández-Martínez et al., 2015). Therefore, under such conditions, plants may act as a significant pathway through which Hg enters terrestrial ecosystems. The evaluation of Hg, particularly MMHg accumulation, in plants from Hg-mining areas is of great concern.

Within the last decade, THg and MMHg in soils, surface waters, and crops, in addition to Hg^0 in the atmosphere, have been widely characterized in the study area of the Wanshan Hg mine (e.g., Horvat et al., 2003; Qiu et al., 2005, 2009; Dai et al., 2013; Yin et al., 2016). Nevertheless, presently, few studies have been conducted regarding the effect of Hg on vegetation (Wang et al., 2011, 2012), particularly the wild species growing vigorously at Hg-enriched wastelands. The biomonitoring of THg and MMHg in the study area has concentrated mostly on agricultural crops consumed by humans, such as rice (Qiu et al., 2008, 2012a, b; Zhang et al., 2010), with a general lack of attention directed to THg and MMHg in naturally dwelling plants, which are likely playing an important role in Hg biomagnification in local terrestrial food chains (Abeysinghe et al., 2017). Therefore, the concentrations of both THg and MMHg in the wild plant species must be determined. Furthermore, if the species that effectively accumulate THg and/or MMHg can be identified, those species could be candidates for phytoremediation of Hg-contaminated soil.

To obtain primary information on the concentrations of THg and MMHg in the plant species growing at Hg-enriched wastelands in the Wanshan mining region was the aim of the present work. We also estimated the soil-to-root transfer efficiency of THg and MMHg in plant species to contribute to the understanding of THg and MMHg in the plant-soil ecosystem. Finally, species were evaluated for their feasibility for phytoremediation of Hg-contaminated soil.

2. Materials and experimental methods

2.1. Study area

The Wanshan District (109°07′–109°24′E; 27°24′–27°38′N) is in eastern Guizhou Province, southwestern China (Fig. 1). The annual average temperature and precipitation are 13.4 °C and 1300 mm, respectively. The agrotypes consist of yellow, red, and paddy soils. The primary minerals in the Wanshan Hg mine are cinnabar, metacinnabar, and elemental Hg. The cinnabar ore is associated with sphalerite, pyrite, and stibnite. Intensive cinnabar ore mining and retorting in Wanshan occurred for 630 years and ceased in 2004 (Qiu et al., 2005). Large quantities of mine-waste calcines were introduced into the surrounding area, producing substantial wastelands. Because of inefficient retorting processes, mine-waste calcines are enriched in secondary Hg compounds, such as metacinnabar, Hg sulfide, Hg chloride, Hg oxide, and elemental Hg, which are water-soluble and can be readily released into nearby sites via leaching processes (Biester et al., 1999; Kim et al., 2004). Because of the large reserves of cinnabar ores and elemental Hg outputs, Wanshan once was termed the “Mercury Capitol” of China.

Four wastelands, Wukeng (WK), Sikeng (SK), Shibakeng (SBK), and Gouxi (GX), were selected for the investigation of THg and MMHg in wild plants. The wastelands of SK, WK, and SBK experienced long-term, intensive cinnabar ore mining and retorting. In brief, SK is 0.8 km southwest of the town of Wanshan, and approximately 31.33 million cubic meters of mine-waste calcines were introduced nearby. WK is 2.5 km northeast of Wanshan, and approximately 44.5 million cubic meters of mine-waste calcines were introduced nearby. SBK is 2.5 km north of Wanshan, and approximately 2.83 million cubic meters of mine-waste calcines were introduced nearby. GX is an abandoned artisanal cinnabar ore mining and retorting site and used a mercuric chloride catalyst to recycle Hg. Calcines and catalyst wastes were observed at the sampling sites. All sampled areas were of barren wastelands, which were away from the water and characterized by alkaline pH, drought and high concentrations of Hg.

2.2. Sampling and analyses

2.2.1. Sampling of plants and soils

2.2.1.1. Plants and corresponding rhizosphere soil sampling. Plants were randomly collected from the wastelands of WK, SK, SBK, and GX during April 5–8, 2015, using a regular sampling grid of 5 m × 5 m. Within each sampling unit, a final sample consisted of three individuals of the same species and similar size. A total of 259 samples were collected during the sampling campaign. After collection, plant samples were in situ separated into roots and aerial shoots using stainless scissors after being washed with water from rivers adjacent to the sampling site. All roots and shoots were separately put into polyethylene bags and stored in coolers (+4 °C) and then shipped to the laboratory within 24 h. In the laboratory, all samples were thoroughly washed with tap water and then cleansed three times with deionized water (DI). An ultrasonic cleaning machine (JP040S; Shenzhen, China) was applied during the DI washing process to exclude adsorption of fine particles on plant tissues. Before grinding to a fine powder, the samples were lyophilized at −50 °C. All powdered samples were stored in polyethylene bags and sealed until analysis.

Corresponding rhizosphere soil of plants were simultaneously collected and stored in polyethylene bags to avoid cross contamination. In the laboratory, soil samples were air-dried at room temperature and then ground in a ceramic disc mill through a 200 mesh for analysis.

2.2.1.2. Plant diversity survey. A quadrat of 1.0 m × 1.0 m was selected for the plant species diversity survey. For each wasteland, a total of 10 quadrats were selected randomly to record individual numbers of all species. The total number of a plant species found in one quadrat was considered the “$Individual\ Plant\ Species_{number}$,” and the total number of quadrats that had a similar plant species was

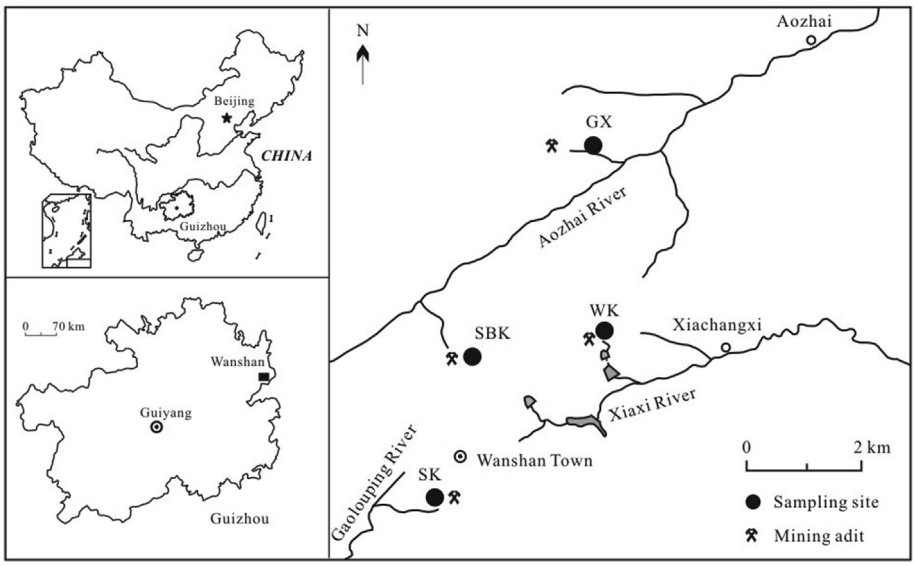

Fig. 1. Map of Wanshan mercury mine and sampling sites.

the "*Individual Plant Species*$_{frequency}$." The dominance values of plant species were calculated as follow:

$$RD(\%) = \frac{Individual\ Plant\ Species_{number}}{All\ Plant\ Species_{number}} \times 100 \quad (1)$$

$$RC(\%) = \frac{Individual\ Plant\ Species_{coverage}}{All\ Plant\ Species_{coverage}} \times 100 \quad (2)$$

$$RF(\%) = \frac{Individual\ Plant\ Species_{frequency}}{All\ Plant\ Species_{frequency}} \times 100 \quad (3)$$

$$DD\ (\%) = \frac{RD + RC + RF}{3} \quad (4)$$

where

RD is the Index of relative density
RC is the Index of relative coverage
RF is the Index of relative frequency
DD is the Dominance degree of THg and MMHg

2.2.2. Analyses

2.2.2.1. Plants. For plant THg analysis, approximately 0.5–1.0 g (accurate to 0.0001) of dry sample was digested using a fresh mixture of HNO_3 and H_2SO_4 (4:1, *v*/*v*) in a water bath at 95 °C for 3 h; then, 5 mL of DI and 0.5 mL of BrCl were added, and the sample was digested for another 30 min before finally bringing the digestate to a fixed volume of 50 mL with DI. After 24 h, 400 μL of $NH_2OH{\cdot}HCl$ was added, and the liquid supernatant with a volume of 5 mL was put into a bubble bottle; then, 400 μL of $SnCl_2$ was added for the THg determination via atomic absorption spectroscopy (AAS, F732-V; Shanghai Huaguang, China) (Qiu et al., 2008).

For MMHg analysis, approximately 0.3–0.5 g (accurate to 0.0001) of dry samples was weighed into Teflon tubes and digested using 25% KOH-methanol in a water bath at 75 °C for 3 h. Then, 1.5 mL of concentrated HCl was added to neutralize and acidify the solution. Ten milliliters of dichloromethane (CH_2Cl_2; HPLC/Spectro Tedia, USA) was added to the digestate followed by shaking for 30 min and then separation. The solvent phase CH_2Cl_2 was collected into a 50 mL Teflon bottle. Approximately 30 mL of DI was added to the solvent phase, and the CH_3HgCl in the samples was back-extracted into water, and approximately 10 mL was removed for measurement using gas chromatography-cold vapor atomic fluorescence spectrometry (GC-CVAFS; Brooks Rand Model III, Seattle, USA) according to US EPA Method 1630 (US EPA, 2001; Liang et al., 1994, 1996). The method requires a progressive sequence of distillation, addition of 2 M acetate buffer, ethylation with 1% sodium tetraethylborate, pure and trap of methylethylmercury onto Tenax traps, and thermal desorption.

2.2.2.2. Soil. For soil THg analysis, approximately 0.1–0.3 g (accurate to 0.0001 g) of sample was weighed into plastic tubes. Then, 5 mL of DI and 5 mL of a mixed solution of HCl and HNO_3 (3:1, *v*/*v*) were added. The samples rested for 5 min, and then 1 mL of BrCl was added for a water bath digestion at 95 °C for 3 h (Meng et al., 2016). After leaving the digestate for 24 h, 400 μL of $NH_2OH{\cdot}HCl$ was added to remove the free halogens, and then, samples were brought to a fixed volume of 50 mL with DI. Approximately 5 mL of digestate volumes was taken for THg analysis similar to the method used for plants.

For soil MMHg determination, approximately 0.3–0.4 g (accurate to 0.0001) of soils was weighed into plastic tubes. Next, 1 mL of 2 mol/L $CuSO_4$ and 4 mL of concentrated HNO_3:H_2O = 1:3 (*v*/*v*) were added, and 5 mL of ultra-pure CH_2Cl_2 was added to extract the CH_3HgCl into the solvent. Afterward, the extract was transferred and weighed, and then the CH_3HgCl was back-extracted to the water phase, and the extract was brought to a fixed volume of 50 mL with DI (Liang et al., 1994, 1996, 2004). Approximately 5 mL aliquots were taken for GC-CVAFS analysis according to US EPA Method 1630 (US EPA, 2001).

For soil pH and EC measurements, approximately 10 g of soil was weighed into plastic vials, and 25 mL of DI was added, mixed for 2 min, and then set for 30 min (Chinese National Standard Agency, 1988). Soil pH was determined using a pH meter (PHS-2E; Shanghai, China). For soil organic matter (OM), approximately 0.5–1.0 g of soil was weighed into colorimetric tubes, $K_2Cr_2O_7$/H_2SO_4 was added and then a water bath-potassium dichromate volumetric method was used for measuring (Lu, 2000).

The mineralogical composition of samples was determined using X-ray diffraction (XRD). The XRD patterns were recorded using a diffractometer (Model: Empyrean) using nickel-filtered Cu Kα

radiation (λ = 1.54178 Å). The data were collected in a 2θ range of 4.1–60° in a continuous scanning mode with a 0.026° step size and a counting time of 30 s per step. The working voltage and current were 40 kV and 40 mA, respectively. The semi-quantitative analysis of the specimens was conducted using the K-value method.

2.3. QA/QC

Data quality control for THg and MMHg analyses was by working standard curve, blanks, duplicates, matrix spikes and certified reference materials of GBW10020, TORT-2, GBW07405, and ERM-CC580. The basic information on certified reference materials is presented in Supplemental Data, Table S1.

Briefly, for plant THg, the measured value of Hg in citrus leaves of GBW10020 was 150 ± 4.1 ng/g (n = 5), which was comparable to the reference value 150 ± 13 ng/g. Recoveries on matrix spikes of THg in plant samples were in the range 91–118%. For plant MMHg, the measured value of MMHg in lobster hepatopancreas of TORT-2 was 155 ± 25 ng/g (n = 5); whereas the reference value was 152 ± 13 ng/g. For soil THg, an average THg concentration of 310 ± 20 ng/g (n = 6) in yellow red soil of GBW07405 was obtained, which was comparable to the certified value of 290 ± 40 ng/g. For soil MMHg, estuarine sediment of ERM-CC580 was determined, and the obtained MMHg concentration of 73.5 ± 5.0 ng/g (n = 6) confirmed the certified value of 75.5 ± 3.7 ng/g.

2.4. Enrichment factor calculations

The bioconcentration factors (BCFs) between soil and root were calculated (Ghosh and Singh, 2005; Yoon et al., 2006; Ye et al., 2009) to evaluate both THg and MMHg migration in the soil-plant system. At high BCF values, the migration of THg and MMHg from soil to plant is easier. The BCFs were calculated as follow:

$$BCFs = \frac{C_{root}}{C_{soil}}$$

where

C_{root} is the Concentration of THg and MMHg in roots
C_{soil} is the Concentration of THg and MMHg in soils

3. Results and discussion

3.1. Plants' characterization

3.1.1. Composition

A total of 259 plants belonging to 49 species in 29 families were found in the present study, including Pteridophyta, Monocotyledons, and Dicotyledons. The Pteridophyta consisted of three species: *Eremochloa ciliaris* of Blechnaceae, *Cibotium barometz* of Dicksoniaceae and Woodwardia, and *Equisetum ramosissimum* of Equisetaceae, belonging to three families. The Monocotyledons included four species: *Arthraxon hispidus* of Gramineal arthraxon, *Imperata cylindrica* of Cogon, *Neyraudia reynaudiana* of Genus type, and *Allium tuberosum* of Allium, belonging to two families. Other plants were classified into 39 species, among which the dominant family of plants was the Feverfew, consisting of 18 species and accounting for 31.6% of plants. The herbaceous plants were both annuals and perennials, accounting for 49.1% and 33.9%, respectively.

The naturally growing plants on the wastelands were exotic and exhibited the capability of migration and tolerance of both barren situations and Hg contamination. In the present study, most species growing on the wastelands were heliophytes and exhibited adaptive capabilities to the dry and barren conditions. The high distribution proportionally of Composita and Polygonaceae might be due to their widespread occurrence and tolerance of nutrient-poor soils (Conesa et al., 2007).

3.1.2. Dominance degree

A wide variability of species community dominance was observed at GX, SBK, SK, and WK, ranging from 1.9 to 12%, 3.5 to 25%, 2.1 to 14%, and 1.0 to 13%, respectively (Table S3). Eight species, *Eremochloa ciliaris*, *Sonchus oleraceus*, *Buddleja lindleyana, Plantago asiatica, Equisetum ramosissimum*, *Herba artimisiae, Rumex acetosa,* and *Houttuynia crdata*, exhibited a high degree of dominance, ranging between 10.5 and 25% for their peak values, of which *E. ciliaris* showed the highest average value of 16 ± 6.1% in the study area.

Data for those eight species with high degrees of dominance identified in the present study indicated their strong adaptabilities to Hg-enriched wastelands. Plants with high dominances are regarded pioneer species for the natural vegetation restoration of wastelands characterized by nutrient deficiencies, toxic element contaminations, and acidic/alkaline conditions (Shaw, 1989; Baker, 1987; Parraga-Aguado et al., 2014). For the study area, the eight adaptively dominant species might be selected as potential pioneer plants for vegetation restoration or phytoremediation.

3.1.3. Tolerant species

To identify the tolerant species, cluster analysis was selected for plant classification according to density. Based on data of plant dominance degree, the Ward method of cluster analysis was applied, automatically generating thresholds (Ts) for the classification criteria of a cluster when the difference between the groups was small and the distance between the groups was obvious (Tang and Feng, 2006; He, 2008). The results suggested that plant tolerance was divided into four grades with Ts values of 2.62, 4.46, 2.82, and 3.37 at GX, SK, WK and SBK, respectively (Fig. 2; Table S4). The plants with a high degree of dominance were defined as tolerant species.

The dominant species *E. ciliaris*, *B. lindleyana*, *E. ramosissimum, H. artimisiae, P. asiatica,* and *S. oleraceus* were identified as tolerant species in this study. The tolerant plants at GX consisted of *E. ciliaris, H. artimisiae* and *S. oleraceus*; with *E. ciliaris, B. lindleyana, P. asiatica* and *S. oleraceus* tolerant at SBK; *E. ciliaris* and *E. ramosissimum* at SK, and *E. ciliaris* at WK. These six species from the study area showed the highest abundances, which indicated their tolerance capabilities in Hg-enriched environments. These species that thrived in the wastelands can be selected as candidates for vegetation restoration or phytoremediation of Hg when they have high bioaccumulation of Hg.

3.2. Rhizophere soil THg and MMHg

In the present study, pH values in soil samples ranged from 6.3 to 10.8 with an average of 8.37, exhibiting an alkaline condition. The highest average pH value of 9.0 was recorded at SK and the lowest average pH value of 8.0 was recorded at GX. Both WK and SBK showed average values of 8.2. The OM in the soils was low and averaged 3.3%, ranging from 0.033 to 13%. GX and SK exhibited the highest and lowest values of OM, 5.4% and 2.5%, respectively. According to the X-ray diffraction analysis data, soil samples showed abundant quartz, calcite, dolomite, orthoclase, and muscovite. Small amounts of marcasite, aragonite, and phosphuranylite were observed at SK and pyrite at SBK. At GX, however, the marcasite component was high and reached 24% (see Supplemental Data, Fig. S1 and Table S2).

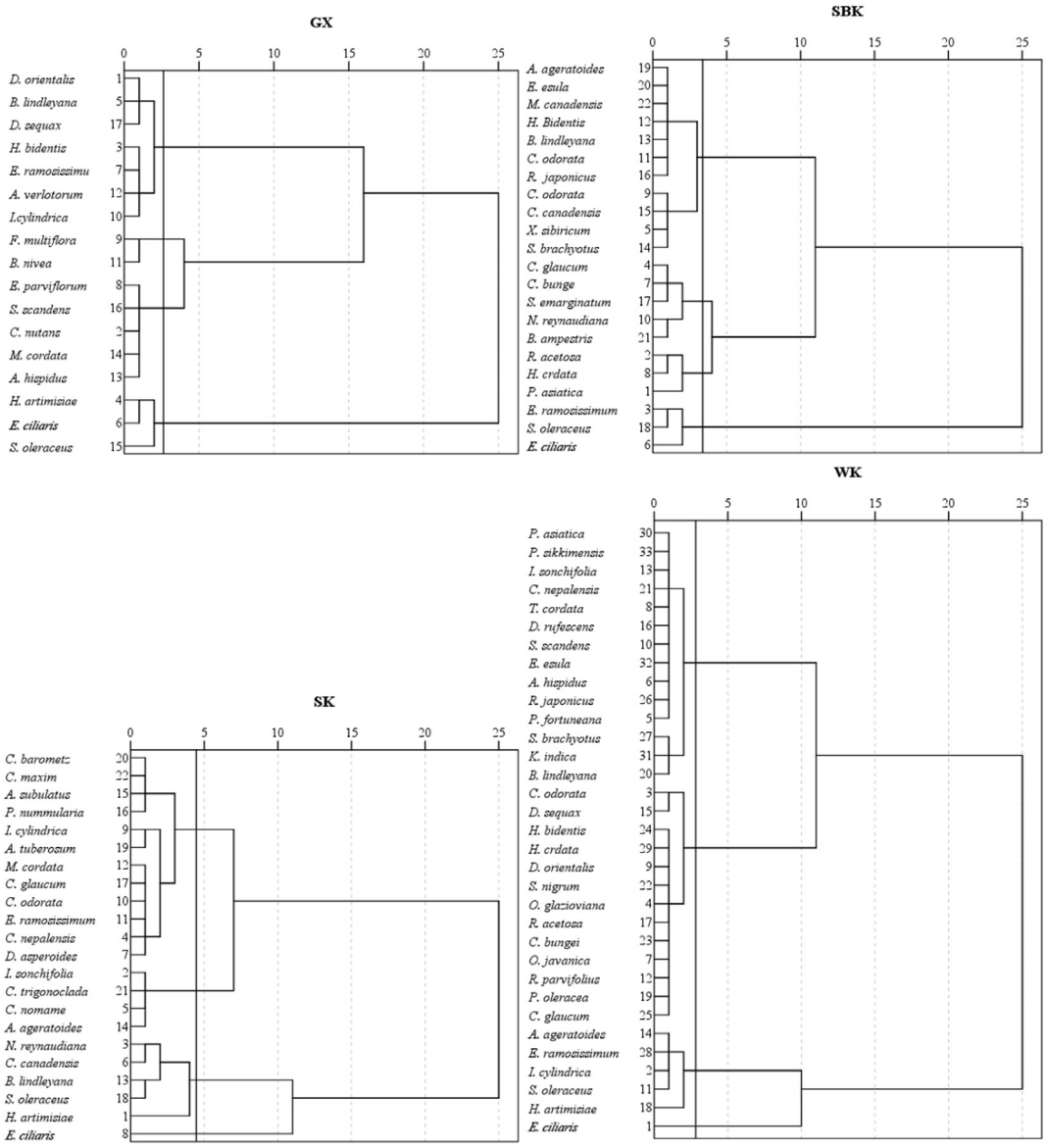

Fig. 2. Hierarchical cluster analysis diagram of tolerant plants in study areas.

Concentrations of THg and MMHg in rhizosphere soils are shown in Table 1. THg concentrations in soil samples ranged from 0.74 to 1440 μg/g with an average of 97 ± 180 μg/g. GX soil THg exhibited the highest average of 210 ± 375 μg/g with a range of 0.81–1440 μg/g. An average of 34 ± 29 μg/g with a range of 1.6–120 μg/g was recorded at SK; an average of 79 ± 91 μg/g with a range of 3.0–450 μg/g at WK; and an average of 110 ± 120 μg/g with a range of 0.74–479 μg/g at SBK. The highest concentration of soil THg was observed at GX, most likely due to the inefficient retorting process with an approximately 70% recovery of historic artisanal Hg mining activities (Li et al., 2013). Our data are close to the results for soils collected from the world's largest Hg mines (e.g., Molina et al., 2006; Gosar and Žibret, 2011; Fernández-Martínez et al., 2015) and as expected, are much higher than the uncontaminated background values of ~0.01–0.5 μg/g (Senesi et al., 1999; Beckers and Rinklebe, 2017). Mine-waste calcines formed under high temperatures usually contain a significant quantity of Hg-enriched secondary minerals (Rytuba, 2003), which might explain the elevated, high THg concentrations in the wasteland soils.

Soil MMHg ranged widely from 0.41 to 820 ng/g with an average of 14 ± 62 ng/g for all samples. The soils exhibited the highest average MMHg of 51 ± 150 ng/g at GX and the lowest average MMHg of 5.4 ± 6.2 ng/g at SBK. The average concentrations of MMHg in soil in the present study were lower than those observed in other Hg mining regions, such as the Alaskan Hg mines (Bailey et al., 2002), the Almadén Hg mine (Higueras et al., 2003, 2006), the Idrija Hg mine (Kocman et al., 2004), the Haliköy Hg mine (Gemici et al., 2009), and the La Soterrañ and Los Rueldos Hg mines (Fernández-Martínez et al., 2015). However, an abnormally high value reaching up to 820 ng/g was recorded at GX. Generally, MMHg in soil is affected by the bioavailable Hg form and soil conditions, such as pH, temperature, oxidation-reduction potential and OM (Ullrich et al., 2001; Amirbahman et al., 2002; Frohne et al., 2012; Beckers and Rinklebe, 2017). The artisanal Hg mining at GX may have led to amounts of elemental Hg emitted into the atmosphere, resulting in high atmospheric Hg deposition in the surrounding area. Such newly deposited Hg is more bioavailable and ready for methylation in soil with low pH (Bailey et al., 2002; Meng

Table 1
THg and MMHg concentrations in plants and rhizosphere soil collected from study areas (μg/g for THg, ng/g for MMHg).

Species	Plant								Soil			
	THg				MMHg				THg		MMHg	
	Root		Aboveground		Root		Aboveground					
	Range	Mean ± SD	Range	Mean ± SD	Range	Mean ± SD	Range	Mean ± SD	Range	Mean ± SD	Range	Mean ± SD
Allium tuberosum	2.1–2.2	2.2 ± 0.063	0.39–0.40	0.40 ± 0.004	1.7–1.8	1.8 ± 0.09	5.9–6.1	6.0 ± 0.11	108–120	110 ± 7.8	19–20	20 ± 1.1
Arthraxon hispidus	120–140	130 ± 9.4	42–98	70 ± 39	83–87	85 ± 3.2	24–25	25 ± 0.81	438–460	450 ± 14	61–820	440 ± 540
Aster ageratoides	0.32–3.4	1.8 ± 1.7	0.58–13	6.3 ± 6.7	0.47–1.9	1.1 ± 0.76	2.3–4.5	3.2 ± 1.1	9.0–31	19 ± 11	0.54–2.1	1.4 ± 0.68
Aster subulatus	1.4–1.5	1.5 ± 0.10	0.41–0.43	0.42 ± 0.01	13–15	14 ± 0.85	10.5–11.3	11 ± 0.55	3.0–3.1	3.0 ± 0.078	0.74–0.85	0.80 ± 0.08
Brassica ampestris	0.094–0.10	0.10 ± 0.006	1.7–2.5	2.2 ± 0.43	0.59–0.93	0.79 ± 0.18	0.38–0.59	0.50 ± 0.11	9.3–63	29 ± 29	4.6–34	16 ± 15.8
Buddleja lindleyana	0.30–56	8.5 ± 19	0.36–28	5.3 ± 9.3	0.73–5.4	2.8 ± 2.2	0.81–3.0	2.0 ± 1.1	6.8–480	98 ± 160	0.79–240	32 ± 84
Buddleja officinalis	0.30–0.81	0.52 ± 0.25	0.50–3.3	1.4 ± 1.1	0.73–1.8	1.2 ± 0.52	2.6–3.0	2.8 ± 0.20	1.2–89	32 ± 37	1.0–6.4	2.9 ± 2.1
Campylotropis trigonoclada	0.91–0.95	0.93 ± 0.034	0.67–0.75	0.71 ± 0.054	n.a.	0.83	n.a.	1.0	32–53	43 ± 15	3.2–5.4	4.3 ± 1.5
Cassia nomame	0.52–0.79	0.66 ± 0.19	0.38–0.63	0.50 ± 0.18	1.9–2.5	2.2 ± 0.48	0.27–1.7	0.99 ± 1.0	5.3–39	22 ± 24	0.57–2.3	1.4 ± 1.2
Chenopodium glaucum	0.40–0.48	0.44 ± 0.058	0.42–0.43	0.43 ± 0.009	0.81–0.83	0.82 ± 0.011	0.27–0.29	0.28 ± 0.017	2.0–4.0	3.0 ± 1.4	2.0–4.1	3.0 ± 1.4
Chromolaene odorata	0.43–6.2	1.5 ± 1.9	0.52–1.9	1.2 ± 0.50	0.25–4.3	1.8 ± 1.6	0.79–3.6	1.7 ± 1.1	0.81–350	97 ± 120	1.3–19	7.2 ± 6.2
Cibotium barometz	1.7–1.8	1.7 ± 0.044	3.6–3.7	3.6 ± 0.075	0.22–0.25	0.24 ± 0.02	0.61–0.68	0.65 ± 0.05	34–36	35 ± 1.4	21–23	22 ± 1.5
Cirsium japonicum	4.8–5.2	5.0 ± 0.24	3.7–3.8	3.8 ± 0.01	4.0–4.2	4.1 ± 0.18	0.42–0.45	0.44 ± 0.02	1390–1440	1420 ± 41	41–44	42 ± 1.8
Clerodendrum bunge	0.29–74	22 ± 34	0.34–9.4	3.0 ± 4.2	0.44–3.8	1.6 ± 1.3	0.38–2.1	1.1 ± 0.66	62–830	330 ± 340	2.2–61	20 ± 28
Conyza canadensis	0.11–4.6	1.5 ± 1.3	0.63–2.8	1.2 ± 0.60	0.37–12	2.9 ± 3.5	0.23–5.0	2.1 ± 1.5	3.1–410	140 ± 170	0.90–32	8.9 ± 19
Coriaria nepalensis	2.6–4.1	3.4 ± 1.0	1.7–2.0	1.8 ± 0.19	0.25–0.43	0.34 ± 0.13	0.35–0.51	0.43 ± 0.11	32–50	41 ± 13	1.4–2.5	2.0 ± 0.77
Corydalisedulis maxim	0.26–0.28	0.27 ± 0.008	0.86–0.87	0.87 ± 0.012	6.0–7.0	6.5 ± 0.68	5.1–5.2	5.1 ± 0.01	18–19	18 ± 0.77	9.9–11	11 ± 0.90
Cyclosorus acuminatus	1.3–1.4	1.3 ± 0.06	2.8–3.9	3.4 ± 0.77	1.3–1.5	1.4 ± 0.15	1.4–1.6	1.5 ± 0.13	40–41	41 ± 0.25	3.2–3.5	3.3 ± 0.22
Debregeasia orientalis	1.2–3.6	2.4 ± 1.7	1.2–1.3	1.3 ± 0.007	n.a.	7.2	n.a.	5.5	53–54	54 ± 0.98	4.0–6.4	5.2 ± 1.7
Desmodium sequax	0.73–9.9	3.5 ± 4.2	0.95–5.7	3.2 ± 2.1	0.30–0.39	0.36 ± 0.13	0.26–0.43	0.33 ± 0.09	3.1–12	8.2 ± 3.9	0.43–1.3	0.71 ± 0.41
Equisetum ramosissimum	1.0–29	7.0 ± 11	0.91–3.0	1.7 ± 0.82	2.2–2.6	2.4 ± 0.33	5.0–5.1	5.0 ± 0.09	1.6–67	41 ± 26	0.59–15	5.2 ± 5.3
Eremochloa ciliaris	0.43–63	8.6 ± 14	0.37–106	12 ± 26	0.52–31	6.4 ± 7.4	0.22–31	3.8 ± 5.5	0.79–910	125 ± 210	0.79–30	7.7 ± 7.2
Euphorbia esula	0.41–2.0	0.89 ± 0.62	0.31–1.6	0.66 ± 0.48	0.64–4.6	2.2 ± 1.7	0.41–2.9	1.4 ± 1.1	26–308	83 ± 88	1.5–105	18 ± 32
Fallopia multiflora	0.19–28	7.8 ± 14	0.44–35	14 ± 17	0.69–1.2	0.92 ± 0.33	0.28–0.50	0.39 ± 0.15	42–110	76 ± 27	0.60–50	16 ± 23
Gynura bicolor	0.78–0.82	0.80 ± 0.027	0.80–0.84	0.82 ± 0.026	3.2–3.6	3.4 ± 0.27	1.2–1.4	1.3 ± 0.20	39–41	40 ± 0.83	11.6–12	12 ± 0.38
Herba artimisiae	0.22–42	6.0 ± 11	0.59–17	2.8 ± 4.4	1.0–4.2	2.6 ± 1.2	0.73–6.6	2.5 ± 2.0	3.8–190	65 ± 74	0.49–34	7.9 ± 8.6
Herba bidentis	0.86–6.3	3.1 ± 2.0	0.60–2.0	1.1 ± 0.56	0.32–1.9	0.91 ± 0.71	0.18–0.88	0.39 ± 0.33	3.3–15	9.1 ± 4.6	0.41–4.0	2.0 ± 1.4
Houttuynia crdata	0.75–3.2	1.5 ± 0.81	0.59–2.6	1.8 ± 0.72	0.19–4.7	2.6 ± 1.5	0.28–2.6	1.3 ± 0.83	3.2–250	86 ± 72	2.4–19	7.2 ± 6.3
Imperata cylindrica	2.6–8.0	5.6 ± 3.8	0.87–1.0	0.96 ± 0.13	2.4–19	11 ± 11	2.7–3.1	2.9 ± 0.30	11–82	46 ± 50	2.8–5.2	4.0 ± 1.7
Ixeris sonchifolia	26–98	62 ± 51	18–22	20 ± 3.1	1.1–6.4	3.7 ± 3.8	1.6–2.0	1.8 ± 0.27	45–82	64 ± 26	7.9–11	9.5 ± 2.3
Macleaya cordata	0.61–0.72	0.68 ± 0.063	0.35–2.2	0.98 ± 1.1	0.26–2.2	1.3 ± 0.96	0.53–0.97	0.79 ± 0.23	4.4–39	18 ± 19	2.2–5.6	4.0 ± 1.7
Mentha canadensis	0.53–1.5	0.93 ± 0.47	0.65–1.3	0.91 ± 0.35	0.61–2.5	1.5 ± 0.97	0.75–1.9	1.2 ± 0.61	5.6–110	74 ± 60	3.0–3.9	3.6 ± 0.51
Neyraudia reynaudiana	0.31–2.5	1.2 ± 0.81	0.37–1.2	0.76 ± 0.38	0.32–4.6	2.5 ± 3.1	0.68–1.2	0.97 ± 0.40	0.87–6.1	3.2 ± 2.1	0.87–5.7	2.7 ± 1.7
Oenanthe javanica	0.82–4.7	1.7 ± 1.7	0.30–2.2	1.0 ± 0.71	0.36–1.7	1.0 ± 0.66	0.30–3.4	1.8 ± 1.5	32–77	51 ± 20	1.5–8.1	4.9 ± 3.2
Oenothera glazioviana	2.8–17	9.9 ± 10	4.2–6.2	5.2 ± 1.4	1.9–3.1	2.5 ± 0.89	1.3–2.5	1.9 ± 0.84	46–280	165 ± 170	2.3–6.2	4.2 ± 1.8
Onchus brachyotus	0.46–0.48	0.47 ± 0.005	1.9–2.0	2.0 ± 0.026	0.69–0.74	0.72 ± 0.04	1.8–1.9	1.8 ± 0.03	37–40	38 ± 1.8	3.1–3.8	3.4 ± 0.47
Plantago asiatica	0.53–0.88	0.61 ± 0.13	0.37–0.95	0.53 ± 0.21	0.28–2.1	1.2 ± 0.79	0.40–0.81	0.59 ± 0.19	8.0–260	170 ± 95	2.0–6.2	4.0 ± 1.8
Portulaca oleracea	0.70–0.96	0.82 ± 0.13	0.71–0.96	0.86 ± 0.13	5.1–5.8	5.5 ± 0.34	0.06–2.6	1.7 ± 1.4	47–87	73 ± 22	2.2–10	5.3 ± 4.5
Pratia nummularia	1.0–1.1	1.1 ± 0.082	1.7–1.8	1.8 ± 0.056	9.1–9.9	9.5 ± 0.52	2.4–2.5	2.5 ± 0.06	24–25	24.5 ± 1.0	7.8–8.4	8.1 ± 0.46
Primula sikkimensis	2.4–2.6	2.5 ± 0.11	6.1–6.4	6.3 ± 0.23	1.9–2.2	2.1 ± 0.22	1.3–1.4	1.4 ± 0.08	150–180	166 ± 18	38–41	40 ± 1.7
Rumex acetosa	0.32–0.52	0.40 ± 0.091	0.26–0.84	0.49 ± 0.27	0.37–0.43	0.40 ± 0.04	0.47–0.76	0.62 ± 0.21	0.74–83	42 ± 47	0.74–4.4	2.3 ± 1.6
Rumex japonicus	0.092–4.8	1.7 ± 2.1	0.19–2.2	1.0 ± 0.70	0.19–5.9	2.6 ± 2.6	0.28–2.6	1.1 ± 0.78	31–105	69 ± 25	1.0–12	4.9 ± 4.5
Sedum bulbiferum	0.59–1.8	1.0 ± 0.64	0.25–0.72	0.51 ± 0.24	0.45–3.0	1.8 ± 1,3	0.34–1.5	0.99 ± 0.60	243–479	350 ± 120	3.6–10	6.0 ± 3.7
Sedum emarginatum	0.49–1.0	0.71 ± 0.24	0.51–0.68	0.58 ± 0.068	1.4–5.6	2.8 ± 1.6	0.33–1.4	0.79 ± 0.39	28–78	46 ± 21	1.8–19	5.0 ± 6.8
Senecio scandens	0.59–0.79	0.69 ± 0.15	0.76–1,1	0.92 ± 0.23	0.81–1.2	1.0 ± 0.20	0.26–0.61	0.43 ± 0.18	3.4–48	26 ± 32	7.3–16	12 ± 6.3
Sonchus oleraceus	0.076–26	3.1 ± 6.3	0.27–13	2.4 ± 3.8	0.25–24	5.7 ± 8.4	0.70–6.3	2.8 ± 2.2	2.7–180	46 ± 51	1.2–530	35 ± 120
Swertia bimaculata	2.4–4.5	3.5 ± 1.5	2.0–2.7	2.4 ± 0.44	0.90–0.99	0.94 ± 0.07	0.60–0.61	0.61 ± 0.01	4.6–26	15 ± 15	1.8–2.9	2.4 ± 0.73
Telosma cordata	0.47–1.5	1.0 ± 0.76	1.6–1.7	1.7 ± 0.12	0.57–0.58	0.58 ± 0.01	0.53–0.56	0.54 ± 0.02	36–89	62 ± 38	4.2–4.5	4.4 ± 0.19
Xanthium sibiricum	0.96–5.3	3.1 ± 2.2	0.62–1.3	1.1 ± 0.36	0.92–6.7	3.8 ± 4.1	3.5–7.0	5.6 ± 2.1	2.9–6.3	4.3 ± 1.8	2.9–8.4	5.0 ± 3.0

n.a.: not available.

Table 2
THg and MMHg in plants and soil from four sampling sites at Wanshan Hg mining region, southwestern China.

Site	Plants								Soil			
	THg (μg/g)				MMHg (ng/g)				THg (μg/g)		MMHg (ng/g)	
	Root		Shoots		Root		Shoots					
	Range	Mean ± SD	Range	Mean ± SD	Range	Mean ± SD	Range	Mean ± SD	Range	Mean ± SD	Range	Mean ± SD
GX	0.19–140	21 ± 34	0.37–98	15 ± 25	0.69–87	12 ± 22	0.22–31	4.9 ± 7.9	0.81–1440	210 ± 370	0.60–820	51 ± 150
SBK	0.094–11	1.7 ± 1.9	0.25–3.2	0.98 ± 0.73	0.09–12	1.5 ± 1.8	0.23–6.3	0.94 ± 1.0	0.74–480	112 ± 120	0.74–34	5.4 ± 6.2
SK	0.076–8.0	1.1 ± 1.2	0.30–5.4	1.4 ± 1.1	0.22–24	3.6 ± 4.9	0.27–11	2.8 ± 2.2	1.6–120	34 ± 29	0.49–32	6.6 ± 6.4
WK	0.092–41	4.8 ± 7.7	0.19–15	2.8 ± 3.1	0.30–6.3	2.9 ± 1.9	0.059–6.9	1.9 ± 1.6	3.1–450	79 ± 91	0.41–105	8.2 ± 16

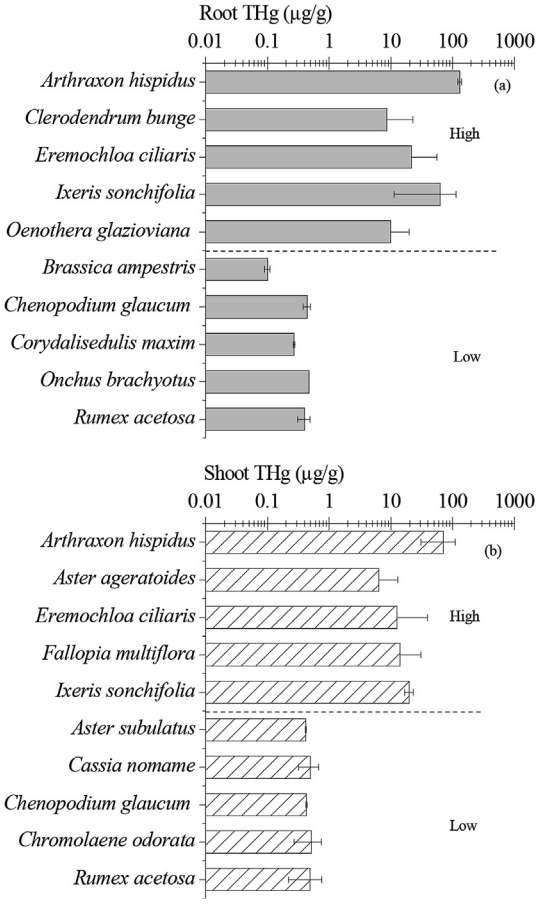

Fig. 3. Total Hg concentrations in plant species grown in wastelands. Among the 49 species analyzed, the top 5 species exhibiting the highest values and the bottom 5 species exhibiting the lowest values in roots (a) and shoots (b) were indicated.

et al., 2011), which could explain the highest levels of MMHg observed at GX.

Ratios of MMHg/THg in soil were usually less than 0.1% with a range of 0.001–3.0% on average, and the peak value was recorded at GX. A significant negative correlation ($r = -0.71$, $p < 0.001$) was observed between THg and the MMHg/THg ratio, and a positive correlation ($r = 0.44$, $p < 0.001$) was observed between THg and MMHg in soils. MMHg/THg ratios decreased with THg concentrations, likely due to the dominant mercuric sulfide compounds in soils from Hg-mining activities (Wang et al., 2012, 2017; Yin et al., 2016), whereas MMHg concentrations increased with THg concentrations, which might be due to the increase in bioavailable Hg forms with increasing amounts of THg. The wide range of soil Hg concentrations observed in the present study may also select different bacterial communities to dominate at different locations, resulting in variations in MMHg production (Beckers and Rinklebe, 2017; Vishnivetskaya et al., 2018). Of the four sampling sites in the present study, the GX soil exhibited higher values of both THg and MMHg than those of the other sites (Table 2), indicating that artisanal smelting activities caused heavy environmental contamination. The most serious issue facing residents is the high concentrations of MMHg, which is readily accumulated and biomagnified in food chains.

3.3. Plant species Hg and MMHg

3.3.1. Roots

Concentrations of THg in the roots of all species exhibited a wide range of 0.076–140 μg/g (Table 1), and the five species with the highest concentrations were *A. hispidus, E. ciliaris, C. bunge, I. sonchifolia,* and *O. glazioviana*, with the peak value of 130 ± 9.4 μg/g on average recorded in *A. hispidus*. By contrast, *B. ampestris*, *C. glaucum*, *C. maxim*, *O. brachyotus*, and *R. acetosa* exhibited the lowest THg concentrations, less than 0.5 μg/g. The lowest value of 0.10 ± 0.006 μg/g on average was observed in *B. ampestris*, which was approximately three orders of magnitude lower than the highest value of *A. hispidus* (Fig. 3a).

Similarly, MMHg concentrations in samples ranged widely from 0.19 to 87 ng/g. Among all species, *A. hispidus* with *A. subulatus, D. orientalis, E. ciliaris, C. maxim, P. nummularia, S. oleraceus, I. cylindrical, X. sibiricum* and *P. oleracea* showed high MMHg concentrations, ranging between 5.5 and 85 ng/g on average. Peak values of 87 and 31 ng/g MMHg were recorded in *A. hispidus and E. ciliaris*, respectively, showing high ability to accumulate MMHg. Approximately 88% of the investigated samples exhibited MMHg concentrations exceeding 1.0 ng/g; only four species, *C. barometz, C. nepalensis, D. sequax,* and *R. acetosa*, exhibited low values of MMHg less than 0.5 ng/g, ranging from 0.24 ± 0.02 to 0.40 ± 0.04 ng/g on average, suggesting a prevalence of MMHg contamination in the surroundings of the wastelands. The analytical data indicated that the fern *E. ciliaris* and *A. hispidus* are capable of extracting MMHg from soils.

Most species that exhibited high THg in roots were growing at GX, indicating significant quantities of bioavailable Hg in the soil. Previous work showed elevated, high total gaseous Hg (TGM) concentrations in the ambient air in the region (Zhao et al., 2016), that were 1–2 orders of magnitude higher than those observed at WK, SK, and SBK, possibly due to newly deposited Hg from atmospheric deposition, which is readily bioavailable (Hintelmann et al., 2002; Mahaffey et al., 2004; Branfireun et al., 2005; Mergler et al., 2007; Gibb et al., 2011), and therefore might play an important role in Hg accumulation for the plants at GX. Ratios of MMHg/THg in roots were usually less than 1%, ranging from 0.0019 to 7.0% with an average of 0.39 ± 0.84%, and the peak ratio value was recorded in *S. oleraceus*. A slightly positive correlation was detected between MMHg and THg ($r = 0.25$, $p = 0.00035$), but a significant negative

correlation was observed between the MMHg/THg ratios and Hg in roots ($r = -0.68$, $p < 0.0001$; Fig. S2).

3.3.2. Shoots

Concentrations of THg in the shoots of all species exhibited a wide range from 0.19 to 106 μg/g. Fig. 3b shows the five species with the highest values and the five species with the lowest values. *Arthraxon hispidus* exhibited the highest average value of 70 ± 39 μg/g of all samples examined in this study. Three other species, *E. ciliaris, F. multiflora,* and *I. sonchifolia*, also exhibited high values of more than 10 μg/g on average, which generally is approximately 2–3 orders of magnitude higher than that observed in plants from uncontaminated areas (usually below 0.1 μg/g) (Lindqvist et al., 1991). Among the high-concentration species, *E. ciliaris* exhibited a peak value of 106 μg/g, suggesting a strong capability of accumulating Hg in its shoots. *Arthraxon subulatus*, *C. nomame, C. glaucum*, *C. odorata*, and *R. acetosa* exhibited low values, with a range from 0.42 to 0.51 μg/g, and the lowest value of 0.42 ± 0.01 μg/g was recorded by *A. subulatus*.

MMHg concentrations in shoots exhibited a wide range of 0.06–31 ng/g, with the highest value of 25 ± 0.81 ng/g on average recorded in *A. hispidus*. The peak MMHg value of 31 ng/g was observed in *E. ciliaris*, indicating its strong ability to accumulate MMHg in both shoots and roots. Approximately 76.5% of the investigated species showed MMHg concentrations exceeding 1.0 ng/g in their shoots. The common phenomenon of high MMHg in plants, particularly their shoots, poses a high risk of health exposure to biota (Jackson et al., 2015; Beckers and Rinklebe, 2017; Abeysinghe et al., 2017). In the present study, MMHg to THg ratios ranged from 0.00042% to 2.6% in shoots, with an average of 0.22 ± 0.36%. The highest ratio was observed in *A. hispidus*, although *A. tuberosum, A. subulatus, E. ciliaris, H. artimisiae,* and *S. oleraceus* also exhibited a high percentage of MMHg to THg in shoots, with peak values greater than 1.0%. No significant positive correlation was detected between MMHg and THg ($r = 0.16$, $p = 0.028$), but a significant negative correlation was observed between the MMHg/THg ratios and THg ($r = -0.71$, $p < 0.0001$; Fig. S2).

Nevertheless, Hg forms in wasteland soils were mostly low-water-soluble cinnabar or meta-cinnabar, and elevated amounts of THg and MMHg were found in area-dwelling plants. Studies show that plants can absorb Hg ions and MMHg from soils via roots and that Hg accumulated at the root apex can be distributed through the vascular system to the leaves (Carrasco-Gil et al., 2013). In this study, significant positive correlations of THg ($r = 0.69$, $p < 0.0001$) and MMHg ($r = 0.49$, $p < 0.0001$) between the roots and aerial shoots of plants were observed (Fig. 4), indicating that roots may play a key role during the process of uptake and transfer of both THg and MMHg from soil to plants.

As expected, the bioavailable soil MMHg exhibited higher positive correlations to root THg ($r = 0.33$, $p < 0.0001$) and shoot THg ($r = 0.38$, $p < 0.0001$; Fig. 5a) than those of soil THg to root THg ($r = 0.29$, $p < 0.0001$) and shoot THg ($r = 0.28$, $p < 0.0001$; Fig. 5b). Soil MMHg also exhibited positive correlations to root MMHg ($r = 0.28$, $p < 0.001$) and shoot MMHg ($r = 0.20$, $p = 0.0044$; Fig. 5c), but no correlations occurred between soil THg and shoots MMHg and soil THg and root MMHg (Fig. 5d). These phenomena confirmed that the Hg of a plant highly depends on bioavailable Hg forms, particularly MMHg in soil, although plants can absorb elemental Hg from the atmosphere (Patra and Sharma, 2000; Millhollen et al., 2006; Fay and Gustin, 2007). Therefore, differences in Hg phytoavailability among the investigated soils could be a key reason for the observed correlations between plant MMHg and soil MMHg or plant THg and soil MMHg.

3.3.3. BCFs of THg and MMHg

Plants exhibited a wide range of BCFs for THg and MMHg, ranging from 0.00028 to 5.5 and from 0.01 to 18, respectively. For THg, eight species, *H. artimisiae, X. sibiricum, H. bidentis, E. ramosissimum, S. oleraceus, I. sonchifolia, N. reynaudiana,* and *E. ciliaris*, exhibited peak values exceeding 1.0, ranging from 1.2 to 5.5, with the highest value recorded in *E. ciliaris*. The difference between the lowest and the highest BCF value was approximately 20,000-fold. For MMHg, sixteen species exhibited peak values exceeding 1.0, ranging from 1.0 to 18, and the highest value was observed in *A. subulatus*. Three species, *H. artimisiae, S. oleraceus,* and *E. ciliaris*, showed high BCFs for both THg and MMHg with peak values exceeding 1.0, indicating their increased ability to accumulate THg and MMHg compared with that of the other species.

Positive correlations between THg BCFs and shoot THg ($r = 0.29$,

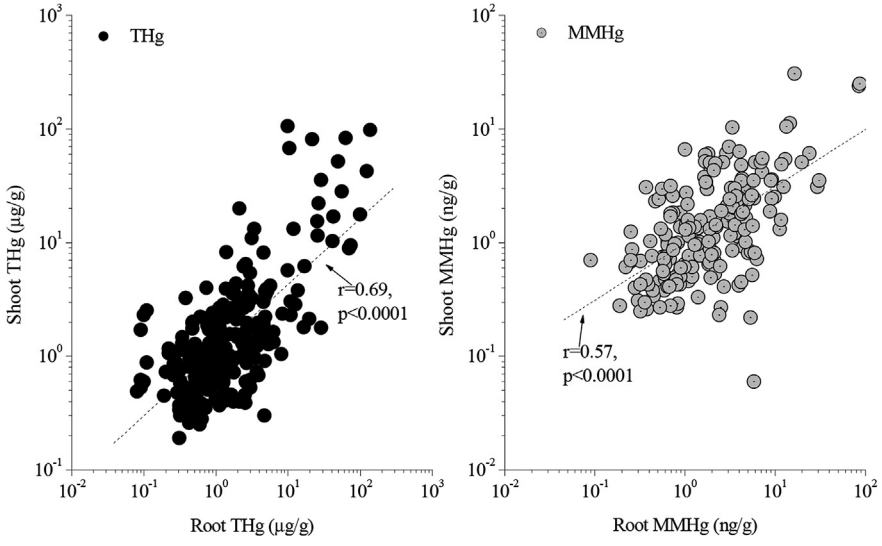

Fig. 4. Plot of correlations between roots and shoots concentrations for THg (left), and MMHg (right).

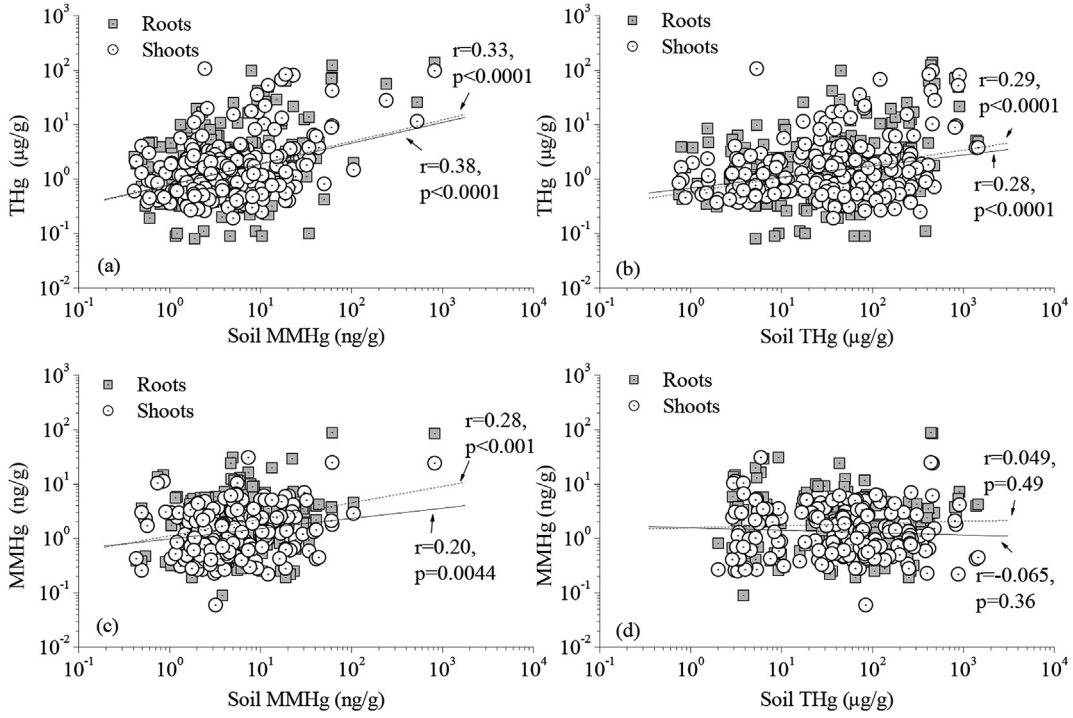

Fig. 5. Scatter diagrams of soil THg vs root THg&MMHg (a) and shoot THg&MMHg (b), and soil MMHg vs root THg&MMHg (c) and shoot THg&MMHg (d).

$p < 0.0001$) and shoot MMHg ($r = 0.34$, $p < 0.0001$) were found. Similarly, a significant positive correlation between the MMHg BCFs and shoot MMHg ($r = 0.34$, $p < 0.0001$) was observed but not a correlation with shoot THg ($r = -0.12$, $p = 0.10$; Fig. S3). Although the roots of plants have "iron plaque" that can effectively prevent Hg ions from soil entering plants (Cavallini et al., 1999; De Sousa et al., 1999; Kalač and Svoboda., 2000), which is considered a natural barrier to prevent Hg absorption by plants (Tiffreau et al., 1995; Gracey and Stewart, 1974; Lindqvist et al., 1991), our results revealed that the capability of root uptake of Hg from soil is an important determinant of both THg and MMHg levels in aerial shoots. The extent of bioaccumulation of Hg in plants is likely dependent on the species (Kalač and Stašková, 1991; Reis et al., 2015).

However, BCFs of plants are dependent not only on the ability of plants to accumulate Hg but also on Hg phytoavailability in different soils (Reis et al., 2015; Beckers and Rinklebe, 2017). The plant species surveyed in the present study grow on soils with different soil characteristics, Hg speciation and therefore phytoavailability. The differences in Hg phytoavailability among the investigated soils could also contribute to the differences in plant Hg levels. Additionally, for a plant species that grows on a soil with high refractory Hg species and high pH, the ability of Hg accumulation may be underestimated (Beckers and Rinklebe, 2017).

3.4. Potential candidates for phytoremediation

Although plants growing on wastelands in the present study exhibited remarkable variation, elevated, high concentrations of THg and MMHg in roots and/or shoots were observed in some species, suggesting those species were particularly capable of accumulating and transferring THg and MMHg. Our data indicated that *A. hispidus, E. ciliaris, F. multiflora,* and *I. sonchifolia* exhibited significantly higher concentrations of THg in shoots and/or roots than those of the other species. Among the four species, both *F. multiflora* and *E. ciliaris* showed higher THg in aerial shoots than that in roots, and *E. ciliaris* not only had a high concentration of THg in shoots but also high concentrations of MMHg in both roots and shoots. The maximum concentration of THg in the shoots of *E. ciliaris* found in the present study exceeded 100 μg/g, exhibiting a peak value of 10 for the shoot/root ratios. The shoots (fronds) also contained the highest concentrations of MMHg, up to 31 ng/g. Compared with *F. multiflora* and *E. ciliaris*, the species *A. hispidus* and *I. sonchifolia* exhibited higher concentrations of THg in roots than those in aerial shoots, whereas *A. hispidus* had the highest concentration of THg in roots of 140 μg/g with a shoot/root ratio of 0.72.

Certain plant species have the ability to accumulate Hg both from the soil and atmospheric sources, and accumulation is not homogeneous among the different organs of a plant (Patra and Sharma, 2000; Rea et al., 2001; Ericksen et al., 2003; Egler et al., 2006; Cosio et al., 2014). Wastelands composed of mine-waste calcines are the primary source for Hg in abandoned Hg mining areas. High levels of THg and MMHg may lead to increased uptake by plants, which in turn can affect the fate of Hg in the environment. In the present study, *A. hispidus* and *E. ciliaris* accumulation of THg exceeded 100 μg/g in the roots and aerial shoots, respectively. We also observed that soil Hg played an important role in plant Hg, indicating that soil Hg rather than atmospheric Hg was the major source for those plants. Because these two species are often found growing in colonies at mine sites or around Hg-retorting sites and exhibit a large biomass, they can be considered prospects for potential application in phytoremediation of Hg-contaminated lands. Particularly *E. ciliaris*, which is a fern and the predominant colonizer of wastelands with a biomass approaching 500 g for shoots and 300 g for roots and is capable of accumulating of THg and MMHg into its fronds, can be considered the best candidate for phytoextraction in the future. At present, although no specific definition exists for a Hg hyperaccumulator, and little is known about Hg hyperaccumulation in plants, we define the fern *E. ciliaris*

as a "Hg hyperaccumulator." Further study on the tolerance of THg and MMHg in the fern is required.

Because the present study was solely conducted in an abandoned Hg mining region, and the most investigated species including *A. hispidus* and *E. ciliaris* were from heavily Hg-contaminated soils of wastelands, the results should be carefully directly extrapolated to other environments. We note, however, that the species *A. hispidus* and particularly the fern *E. ciliaris* are ubiquitous and abundant in subtropical humid climates and can be farmed in arable soils yielding a large annual aboveground biomass. Hence, our findings provide valuable information to help guide future studies of the potential abilities of these two species for Hg phytoremediation in other types of contaminated lands, e.g., the currently widespread Hg-contaminated farmlands caused by excessive use of fertilizers and pesticides, sewage irrigation, and long-term of atmospheric Hg deposition.

4. Conclusions

A total of 259 plant samples belonging to 49 species in 29 families were investigated, of which *E. ciliaris*, *B. lindleyana*, *E. ramosissimum, H. artimisiae, P. asiatica,* and *S. oleraceus* were identified as the dominant Hg-tolerant species. Although THg and MMHg concentrations in plants and rhizosphere soils varied widely, among all species, *A. hispidus* and *E. ciliaris* showed the highest concentrations of THg, greater than 100 μg/g in roots and shoots, respectively, and both exhibited high MMHg in roots and shoots, reaching 88 and 31 ng/g, respectively. Moreover, the highest shoot/root ratio of 10 was recorded in *E. ciliaris*, with its BCF value exceeding 1.0. The bioavailable soil MMHg exhibited higher positive correlations with plant THg than those of soil THg, suggesting differences in Hg phytoavailability among the investigated soils could contribute to the differences in plant Hg levels. Considering THg and MMHg concentrations in aerial shoots and the degree of dominance tolerance, the fern *E. ciliaris* is suggested as a practical phytoremediation candidate and a Hg hyperaccumulator, indicating its potential for phytoextraction of both THg and MMHg at abandoned Hg mining sites. Because of the highest concentrations of THg in roots, *A. hispidus* can be considered a potential candidate for phytostabilization of Hg-contaminated soil. Therefore, the precise characterization of THg and MMHg tolerance and accumulation mechanisms of both *E. ciliaris* and *A. hispidus* will become important in the future.

Acknowledgments

Financial support for this work was provided by the Natural Science Foundation of China (NFSC: 41573135), the Opening Fund of the State Key Laboratory of Environmental Geochemistry (SKLEG2017904). We also appreciate Dr Yong Meng who conducted the X-ray diffraction analysis and data processing.

Appendix A. Supplementary data

Supplementary data related to this article can be found at https://doi.org/10.1016/j.envpol.2018.04.105.

References

Abeysinghe, K.S., et al., 2017. Mercury flow through an Asian rice-based food web. Environ. Pollut. 229, 219–228.
Amirbahman, A., et al., 2002. Association of methylmercury with dissolved humic acids. Environ. Sci. Technol. 36 (4), 690–695.
Bailey, E.A., et al., 2002. Mercury in vegetation and soils at abandoned mercury mines in southwestern Alaska, USA. Geochem. Explor. Environ. Anal. 2 (3), 275–285.
Baker, A.J.M., 1987. Metal tolerance. New Phytol. 106 (s1), 93–111.
Baya, P.A., Van Heyst, B., 2010. Assessing the trends and effects of environmental parameters on the behavior of mercury in the lower atmosphere over cropped land over four seasons. Atmos. Chem. Phys. 10 (17) https://doi.org/10.5194/acp-10-8617-2010.
Beckers, F., Rinklebe, J., 2017. Cycling of mercury in the environment: source, fate, and human health implications: a review. Crit. Rev. Environ. Sci. Technol. 47 (9), 693–794.
Biester, H., et al., 1999. Mercury speciation in tailings of the Idrija mercury mine. J. Geochem. Explor. 65 (3), 195–204.
Bishop, K.H., et al., 1998. Xylem Sap as a pathway for total mercury and methylmercury transport from soil to tree canopy in the boreal forest. Biogeochemistry 40, 101–113.
Branfireun, B.A., et al., 2005. Speciation and transport of newly deposited mercury in a boreal forest wetland: a stable mercury isotope approach. Water Resour. Res. 41 (6), 431–432.
Carrasco-Gil, S., et al., 2013. Mercury localization and speciation in plants grown hydroponically or in a natural environment. Environ. Sci. Technol. 47, 3082–3090.
Cavallini, A., et al., 1999. Mercury uptake, distribution and DNA affinity in durum wheat (*Triticum durum Desf.*) plants. Sci. Total Environ. 243, 119–127.
Chinese National Standard Agency, 1988. Determination of PH Value in Forest Soil. GB7859-87, pp. 171–173 (in Chinese).
Clarkson, T.W., 1993. Mercury: major issues in environmental health. Environ. Health Perspect. 100, 31–38.
Conesa, H.M., et al., 2007. Dynamics of metal tolerant plant communities development in mine tailings from the Cartagena-La Unión Mining District (SE Spain) and their interest for further revegetation purposes. Chemosphere 68 (6), 1180–1185.
Cosio, C., Flück, R., Regier, N., Slaveykova, V.I., 2014. Effects of macrophytes on the fate of mercury in aquatic systems. Environ. Toxicol. Chem. 33 (6), 1225–1237.
Dai, Z., et al., 2013. Assessing anthropogenic sources of mercury in soil in Wanshan Hg mining area, Guizhou, China. Environ. Sci. Pollut. Control Ser. 20 (11), 7560–7569.
De Sousa, M.P., et al., 1999. Rhizosphere bacteria enhance the accumulation of selenium and mercury in wetland plants. Planta 209 (2), 259–263.
Egler, S.G., et al., 2006. Evaluation of mercury pollution in cultivated and wild plants from two small communities of the Tapajós gold mining reserve, Pará State, Brazil. Sci. Total Environ. 368 (1), 424–433.
Ericksen, J.A., et al., 2003. Accumulation of atmospheric mercury in forest foliar. Atmos. Environ. 37 (12), 1613–1622.
Fay, L., Gustin, M.S., 2007. Investigation of mercury accumulation in cattails growing in constructed wetland mesocosms. Wetlands 27 (4), 1056–1065.
Fernández-Martínez, R., Rucandio, I., 2013. Assessment of a sequential extraction method to evaluate mercury mobility and geochemistry in solid environmental samples. Ecotoxicol. Environ. Saf. 97, 196–203.
Fernández-Martínez, R., et al., 2015. Mercury accumulation and speciation in plants and soils from abandoned cinnabar mines. Geoderma 253, 30–38.
Frohne, T., et al., 2012. Biogeochemical factors affecting mercury methlation rate in two contaminated floodplain soils. Biogeosciences 9, 493–507.
Frohne, T., Rinklebe, J., 2013. Biogeochemical fractions of mercury in soil profiles of two different floodplain ecosystems in Germany. Water Air Soil Pollut. 224 https://doi.org/10.1007/s11270-013-1591-4.
Gemici, Ü., et al., 2009. Factors controlling the element distribution in farming soils and water around the abandoned Haliköy mercury mine (Beydağ, Turkey). Appl. Geochem. 24 (10), 1908–1917.
Ghosh, M., Singh, S.P., 2005. A comparative study of cadmium phytoextraction by accumulator and weed species. Environ. Pollut. 133 (2), 365–371.
Gibb, H., et al., 2011. Biomarkers of mercury exposure in two eastern Ukraine cities. J. Occup. Environ. Hyg. 8 (4), 187–193.
Gnamuš, A., et al., 2000. Mercury in the soil-plant-deer-predator food chain of a temperature forest in Slovenia. Environ. Sci. Technol. 34 (16), 3337–3345.
Gosar, M., Žibret, G., 2011. Mercury contents in the vertical profiles through alluvial sediments as a reflection of mining in Idrija (Slovenia). J. Geochem. Explor. 110 (2), 81–91.
Gracey, H.I., Stewart, J.W.B., 1974. Distribution of mercury in Saskatchewan soils and crops. Can. J. Soil Sci. 54 (1), 105–108.
Gray, J.E., et al., 2004. Mercury speciation and microbial transformations in mine wastes, stream sediments, and surface waters at the Almadén mining district, Spain. Environ. Sci. Technol. 38 (16), 4285–4292.
He, X.Q., 2008. Multivariate Statistical Analysis, second ed. Renmin University of China Press, Beijing, pp. 54–60.
Higueras, P., et al., 2003. A first insight into mercury distribution and speciation in soils from the Almadén mining district, Spain. J. Geochem. Explor. 80 (1), 95–104.
Higueras, P., et al., 2006. The Almadén district (Spain): anatomy of one of the world's largest Hg-contaminated sites. Sci. Total Environ. 356 (1), 112–124.
Hintelmann, H., et al., 2002. Reactivity and mobility of new and old mercury deposition in a boreal forest ecosystem during the first year of the METAALICUS study. Mercury Experiment to Assess Atmospheric Loading in Canada and the US. Environ. Sci. Technol. 36 (23), 5034–5040.
Horvat, M., et al., 2003. Total mercury, methylmercury and selenium in mercury polluted areas in the province Guizhou, China. Sci. Total Environ. 304, 231–256.
Jackson, A.K., et al., 2015. Songbirds as sentinels of mercury in terrestrial habitats of eastern North America. Ecotoxicology 24 (2), 453–467.

Kalač, P., Stašková, I., 1991. Concentrations of lead, cadmium, mercury, and copper in mushrooms in the vicinity of a lead smelter. Sci. Total Environ. 105, 109–119.
Kalač, P., Svoboda, L., 2000. A review of trace element concentrations in edible mushrooms. Food Chem. 69 (3), 273–281.
Kim, C.S., et al., 2004. Geological and anthropogenic factors influencing mercury speciation in mine wastes: an EXAFS spectroscopy study. Appl. Geochem. 19 (3), 379–393.
Kocman, D., et al., 2004. Mercury fractionation in contaminated soils from the Idrija mercury mine region. J. Environ. Monit. 6 (8), 696–703.
Kocman, et al., 2011. Distribution and partitioning of mercury in a river catchment impacted by former mercury mining activity. Biogeochemistry 104, 183–201.
Li, P., et al., 2013. Mercury speciation and mobility in mine wastes from mercury mines in China. Environ. Sci. Pollut. Res. 20 (12), 8347–8381.
Liang, L., et al., 2004. Re-evaluation of distillation and comparison with HNO_3 leaching/solvent extraction for isolation of methylmercury compounds from sediment/soil samples. Appl. Organomet. Chem. 18, 264–270.
Liang, L., et al., 1996. Simple solvent extraction technique for elimination of matrix interferences in the determination of methylmercury in environmental and biological samples by ethylation-gas chromatography-cold vapor atomic fluorescence spectrometry. Talanta 43 (11), 1883–1888.
Liang, L., et al., 1994. An improved speciation method for mercury by GC/CVAFS after aqueous phase ethylation and room temperature precollection. Talanta 41 (3), 371–379.
Lindberg, S.E., et al., 2007. A synthesis of progress and uncertainties in attributing the source of mercury in deposition. Ambio 36 (1), 19–32.
Lindqvist, O., 1991. Special issue of first international on mercury as a global pollutant. Water Air Soil Pollut. 56, 1–11.
Lindqvist, O., et al., 1991. Mercury in the Swedish environment-recent research on causes, consequences and corrective methods. Water Air Soil Pollut. 55 pp. xi-261.
Lu, R., 2000. Chemical Analysis Method of Agricultural Soil. China Agriculture Science Press, Beijing, pp. 106–107 (in Chinese).
Lu, Z., et al., 2016. High mercury accumulation in two subtropical evergreen forests in South China and potential determinants. J. Environ. Manag. 183, 488–496.
Mahaffey, K.R., et al., 2004. Blood organic mercury and dietary intake: national health and nutrition examination survey, 1999 and 2000. Environ. Health Perspect. 112 (5), 562–570.
Meng, B., et al., 2011. The process of methylmercury accumulation in rice (*Oryza sativa L.*). Environ. Sci. Technol. 45 (7), 2711–2717.
Meng, B., et al., 2016. The impacts of organic matter on the distribution and methylation of mercury in a hydroelectric reservoir in Wujiang River, Southwest China. Environ. Toxicol. Chem. 35 (1), 191–199.
Menzies, N.W., et al., 2007. Evaluation of extractants for estimation of the phytoavailable trace metals in soils. Environ. Pollut. 145, 121–130.
Mergler, D., et al., 2007. Methylmercury exposure and health effects in humans: a worldwide concern. Ambio 36 (1), 3–11.
Millán, R., et al., 2006. Mercury content in vegetation and soils of the Almadén mining area (Spain). Sci. Total Environ. 368 (1), 79–87.
Millhollen, A.G., et al., 2006. Mercury accumulation in grass and forb species as a function of atmospheric carbon dioxide concentrations and mercury exposure in air and soil. Chemosphere 65 (5), 889–897.
Molina, J.A., et al., 2006. Mercury accumulation in soils and plants in the Almadén mining district, Spain: one of the most contaminated sites on Earth. Environ. Geochem. Health 28 (5), 487–498.
Parraga-Aguado, I., et al., 2014. Usefulness of pioneer vegetation for the phytomanagement of metal(loid)s enriched tailing: grasses vs. shrubs vs. trees. J. Environ. Manag. 133, 51–58.
Patra, M., Sharma, A., 2000. Mercury toxicity in plants. Bot. Rev. 66 (3), 379–422.
Pérez-Sanz, A., et al., 2012. Mercury uptake by *Silene vulgaris* grown on contaminated spiked soils. J. Environ. Manag. 95, S233–S237.
Qiu, G., et al., 2005. Mercury and methylmercury in riparian soil, sediments mine-waste calcines, and moss from abandoned Hg mines in east Guizhou province, southwestern China. Appl. Geochem. 20 (3), 627–638.
Qiu, G., et al., 2008. Methylmercury accumulation in rice (*Oryza sativa L.*) grown at abandoned mercury mines in Guizhou, China. J. Agric. Food Chem. 56 (7), 2465–2468.
Qiu, G., et al., 2009. Mercury distribution and speciation in water and fish from abandoned Hg mines in Wanshan, Guizhou province, China. Sci. Total Environ. 407 (18), 5162–5168.
Qiu, G., et al., 2012a. Environmental geochemistry of an active Hg mine in Xunyang, Shaanxi Province, China. Appl. Geochem. 27 (12), 2280–2288.
Qiu, G., et al., 2012b. Methylmercury in rice (*Oryza sativa L.*) grown from the Xunyang Hg mining area, Shaanxi province, northwestern China. Pure Appl. Chem. 84, 281–289.
Qiu, G., et al., 2013. Environmental geochemistry of an abandoned mercury mine in Yanwuping, Guizhou Province, China. Environ. Res. 125, 124–130.
Rajan, M., et al., 2008. Hg L3XANES study of mercury methylation in shredded *Eichhornia crassipes*. Environ. Sci. Technol. 42 (15), 5568–5573.
Rea, A.W., et al., 2001. Dry deposition and foliar leaching of mercury and selected trace elements in deciduous forest throughfall. Atmos. Environ. 35 (20), 3453–3462.
Reis, A.T., et al., 2015. Extraction of available and labile fractions of mercury from contaminated soils: the role of operational parameters. Geoderma 259, 213–223.
Rytuba, J.J., 2003. Mercury form mineral deposits and potential environmental impact. Environ. Geol. 43 (3), 326–338.
Schwesig, D., Krebs, O., 2003. The role of ground vegetation in the uptake of mercury and methylmercury in a forest ecosystem. Plant Soil 253 (2), 445–455.
Senesi, G.S., et al., 1999. Trace element inputs into soils by anthropogenic activities and implications for human health. Chemosphere 39 (2), 343–377.
Shaw, J., 1989. Heavy Metal Tolerance in Plants: Evolutionary Aspects. CRC Press, Boca Raton, Florida, pp. 95–215.
Shiyab, S., et al., 2009. Phytotoxicity of mercury in Indian mustard (*Brassica juncea L.*). Ecotoxicol. Environ. Saf. 72 (2), 619–625.
Stein, E.D., et al., 1996. Environmental distribution and transformation of mercury compounds. Crit. Rev. Environ. Sci. Technol. 26 (1), 1–43.
Tang, Q.Y., Feng, M.G., 2006. DPS Data Processing System-experimental Design, Statistical Analysis and Model Optimization. Science Press, Beijing, pp. 443–611.
Tiffreau, C., et al., 1995. Modeling the adsorption of mercury (II) on (hydr) oxides: I. Amorphous iron oxide and α-quartz. J. Colloid Interface Sci. 172 (1), 82–93.
Tomiyasu, T., et al., 2012. The distribution of total and methylmercury concentrations in soils near the Idrija mercury mine, Slovenia, and the dependence of the mercury concentrations on the chemical composition and organic carbon levels of the soil. Environ. Earth Sci. 65, 1309–1322.
Ullrich, S.M., et al., 2001. Mercury in the aquatic environment: a review of factors affecting methylation. Crit. Rev. Environ. Sci. Technol. 31 (3), 241–293.
US EPA, 2001. Method 1630: Methylmercury in Water by Distillate, Aqueous Ethylation, Purge and Trap, and CVAFS. Draft January 2001. U.S. Environmental Protection Agency, Office of Water, Office of Science and Technology Engineering and Analysis Division (4303), pp. 1–41, 1200 Pennsylvania Avenue NW, Washington, D.C. 20460.
Vishnivetskaya, et al., 2018. Microbial community structure with trends in methylation gene diversity and abundance in mercury-contaminated rice paddy soils in Guizhou, China. Environ. Sci. Process. Impacts. https://doi.org/10.1039/c7em00558j.
Wang, J., et al., 2011. Mercury distribution in the soil-plant-air system at the Wanshan mercury mining district in Guizhou, Southwest China. Environ. Toxicol. Chem. 30 (12), 2725–2731.
Wang, J., et al., 2012. Implications of mercury speciation in thiosulfate treated plants. Environ. Sci. Technol. 46 (10), 5361–5368.
Wang, J., et al., 2017. Screening of chelating ligands to enhance mercury accumulation from historically mercury-contaminated soils for phytoextraction. J. Environ. Manag. 186, 233–239.
WHO, 1990. Methylmercury. Environmental Health Criteria 101. World Health Organization, International Program on Chemical Safety, Geneva, Switzerland.
Xia, C., et al., 2010. Atmospheric mercury in the marine boundary layer along a cruise path from Shanghai, China to Prydz Bay, Antarctica. Atmos. Environ. 44 (14), 1815–1821.
Ye, M., et al., 2009. Biogeochemical studies of metallophytes from four copper-enriched sites along the Yangtze River, China. Environ. Geol. 56 (7), 1313–1322.
Yin, R., et al., 2016. Distribution and geochemical speciation of soil mercury in Wanshan Hg mine: effects of cultivation. Geoderma 272, 32–38.
Yoon, J., et al., 2006. Accumulation of Pb, Cu, and Zn in native plants growing on a contaminated Florida site. Sci. Total Environ. 368 (2), 456–464.
Zhang, H., et al., 2010. In inland China, rice, rather than fish, is the major pathway for methylmercury exposure. Environ. Health Perspect. 118 (9), 1183–1188.
Zhao, J.T., et al., 2014. Study of mercury resistance wild plants in the mercury mine area of Wanshan district Guizhou Province. Asian J. Ecotoxicol. 9 (5), 881–887 (in Chinese).
Zhao, L., et al., 2016. Mercury methylation in paddy soil: source and distribution of mercury species at a Hg mining area, Guizhou Province, China. Biogeosciences 13, 2429–2440.
Zhu, D.W., et al., 2015. Prediction of methylmercury accumulation in rice grains by chemical extraction methods. Environ. Pollut. 199, 1–9.